

An Exoskeleton for Overhead Work Support Equipped with Pneumatic Artificial Muscles: An Insight on Transmission Design

Original

An Exoskeleton for Overhead Work Support Equipped with Pneumatic Artificial Muscles: An Insight on Transmission Design / Paterna, M., De Benedictis, C., Ferraresi, C.. - ELETTRONICO. - 157:(2024), pp. 543-551. (RAAD 2024 Cluj-Napoca, Romania 5-7 giugno 2024) [10.1007/978-3-031-59257-7_54].

Availability:

This version is available at: 11583/2989166 since: 2024-10-02T08:04:14Z

Publisher:

Springer

Published

DOI:10.1007/978-3-031-59257-7_54

Terms of use:

This article is made available under terms and conditions as specified in the corresponding bibliographic description in the repository

Publisher copyright

Springer postprint/Author's Accepted Manuscript (book chapters)

This is a post-peer-review, pre-copyedit version of a book chapter published in Advances in Service and Industrial Robotics RAAD 2024. The final authenticated version is available online at: http://dx.doi.org/10.1007/978-3-031-59257-7_54

(Article begins on next page)

An exoskeleton for overhead work support equipped with pneumatic artificial muscles: an insight on transmission design

Maria Paterna^[0000-0001-5484-7491], Carlo De Benedictis^{*[0000-0003-0687-0739]} and Carlo Ferraresi^[0000-0002-9703-9395]

Department of Mechanical and Aerospace Engineering, Politecnico di Torino, Turin, Italy
carlo.debenedictis@polito.it

Abstract. Exoskeletons are wearable systems designed to assist human limb movement and reduce human muscle effort. Passive upper-limb exoskeletons are recently spreading in industrial environments to aid workers during long, repetitive overhead tasks. Generally, these devices engage spring systems to counterbalance the gravitational torque about the shoulder joint.

This paper investigates and compares the effects of two different transmissions on the performance of a passive upper-limb exoskeleton based on pneumatic artificial muscles. Simulation results highlight that the different design solutions can either favor a wider range of motion or, alternatively, a better ergonomics and ease of assembling and wearing the device.

Keywords: Passive Exoskeleton, Upper Limb Exoskeleton, Pneumatic Artificial Muscles, Soft Actuators, Wearable Systems.

1 Introduction

Exoskeletons are active or passive devices that, in general, mimic human kinematics to support limb motions and empower the user. Based on the aided human limbs, they can be classified into lower-limb and upper-limb exoskeletons. Generally, the latter must deliver less force and torque, but they are more complex from the kinematic point of view. The primary purpose of a lower-limb exoskeleton is to assist locomotion, to provide stability, and to support user weight. Therefore, the high torque demands usually require electric [1], pneumatic [2], or hydraulic actuators [3]. On the other hand, an upper-limb exoskeleton must ensure a wide range of motion to allow manipulation tasks. Active upper-limb exoskeletons have been employed in rehabilitation to control the movement of physically impaired patients. However, the high number of degrees of freedom (DOF) of the upper limb (9 DOF) and the complexity of actuating and actively controlling each DOF while avoiding the singularities increase the overall footprint, inertia, and power consumption. Therefore, these exoskeletons are typically mounted on a stationary platform [4, 5]. Although some examples of wearable active upper-limb exoskeletons designed to assist workers during

overhead repetitive tasks are present in the literature [6–8], passive exoskeletons exploiting one or multiple springs and a transmission to transform elastic energy into an assistive action are generally preferred in the industrial environment [9–11], aimed at balancing the gravitational torque on the shoulder thus reducing workers’ muscular effort. Springs are commonly employed because of their linear behavior. However, they have a relatively low energy density, and a preload system is required to regulate the exoskeleton’s supporting action.

Alternatively to traditional spring systems, pneumatic artificial muscles (PAMs) might be employed as nonlinear gas springs because of their elastic properties [12, 13]. They have a high power-to-weight ratio and are simple to install, so they have no negative impact on the weight and total size of the device. Moreover, safe human-exoskeleton interaction is ensured by their softness and resemblance to human skeleton muscles. Furthermore, broad customization of the actuator’s response to suit different working tasks is made possible by the availability of PAMs in various sizes as well as thanks to the ability to modify the action level by adjusting the supply pressure. Finally, PAMs may be used in industrial applications since they are low-cost, resistant to high temperatures, thermal gradients, dusty and dirty environments. Despite all these advantageous features, no passive upper-limb exoskeletons currently use PAM for gravity-balancing purposes.

This work is focused on a passive upper-limb industrial exoskeleton based on McKibben PAMs for assisting workers during prolonged overhead tasks. By design, the torque provided by the exoskeleton at the shoulder joint should be as close as possible to the gravitational one. Therefore, a transmission capable of matching PAM nonlinear characteristic to external demand is necessary. This paper focuses on identifying the transmission that optimizes the exoskeleton performance. Two design solutions are presented and discussed. The PAMs are positioned behind the user’s back in both scenarios, and the traction force is transmitted by a cable that slides on a fixed shoulder pad of appropriate profile (configuration A) or wraps on a cam that rotates about the shoulder flexion axis (configuration B). Configuration A has been already presented in a previous work of the authors [13]. The results highlighted high support action (up to 74% of the gravitational torque is provided by the exoskeleton) but a limited range of motion (shoulder flexion between 90° and 120°). This paper tests a different PAM size and optimizes its characteristic parameters (i.e., supply pressure and initial contraction ratio) to expand the range of movement exploited by configuration A. The second solution (configuration B) is also studied and discussed. The numerical simulation results obtained with the two configurations are presented to compare the different performance.

2 Exoskeleton transmission design

A commercial PAM (DMSP-10-350N-RM-CM, FESTO, Germany), with an internal diameter of 10 mm and a nominal length of 350 mm, has been considered in this work, among other options. PAM maximum allowable contraction and pre-tensioning are 25% (≈ 87 mm) and 3% (≈ 10 mm) of the muscle nominal length, respectively.

Fig. 1 illustrates the PAM static characteristic, which can be approximated by Eq. (1) [14]:

$$F = (0.01534p + 130.8)e^{-0.3972k} - 0.02605pk + 0.7911p - 127.1 \quad (1)$$

In Eq. (1), F is the PAM traction force, p is the supply pressure, and k is the contraction ratio.

The PAM force is transmitted by a Dyneema® wire (Braided climax - 200daN, OCKERT, Germany), which is considered inextensible for transmission design purposes. In the following, the different transmission configurations are shown.

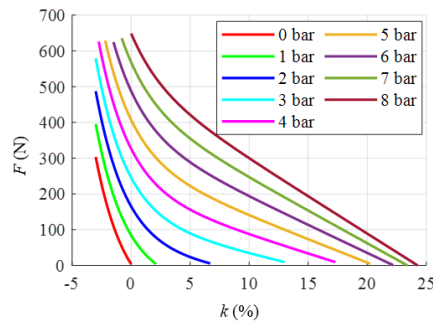


Fig. 1 PAM static characteristics.

2.1 Configuration A: fixed pad-based transmission

Configuration A of the transmission is shown in Fig. 2.

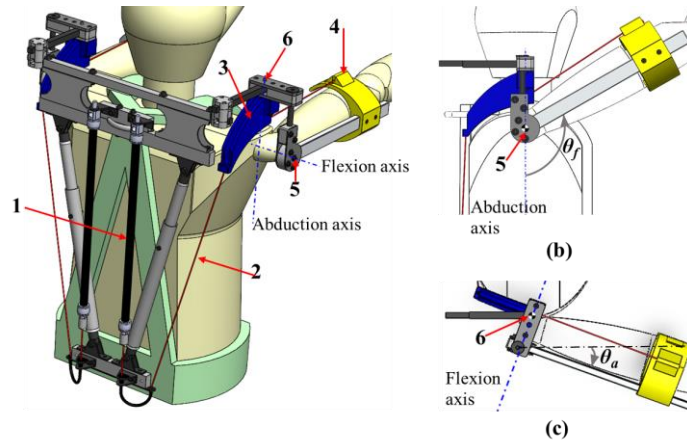


Fig. 2 Configuration A of the transmission implemented into the exoskeleton structure (a); the exoskeleton arm in flexed (b) and abducted (c) positions. θ_f and θ_a are the shoulder flexion and abduction angles, respectively.

Two PAMs (1), one for each arm, are on the back of the user, with the upper ends fastened to the structure and the lower ends joined to a wire (2) that wraps around a shoulder pad (3) and connects to the bracelet (4) that supports the arm of the user. Two revolute joints (5-6) ensure shoulder flexion (Fig. 2(b)) and abduction (Fig. 2(c)).

The shoulder pad profile is designed to approximate the gravitational torque at the shoulder by using the graphical method described in previous works of the authors [12, 13]. The result is shown in Fig. 3a, together with the PAM force lever arm (Fig. 3b) and the muscle stretching with respect to the mounting length (i.e., the length of the muscle in operating conditions when the shoulder flexion angle is 90° , Fig. 3c).

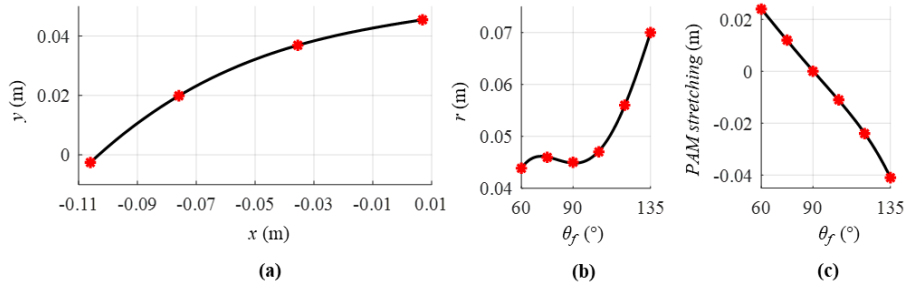


Fig. 3 Shoulder pad profile (a) along with the PAM force lever arm (b) and stretching (c) for shoulder flexion angles between 60° and 135° . The red dots are the data extrapolated from the CAD while the black line is the result of interpolation.

It should be noted that the gravitational torque on the shoulder is maximum for a flexion angle of 90° and decreases both as this angle increases and decreases. On the other hand, the force provided by the PAM has an ever-increasing trend as its length increases. Therefore, the PAM behavior follows the trend of the gravitational torque above 90° , while they are in contrast for lower angles (Fig. 3c).

Since the reduction in gravitational torque above 90° does not accurately match the decrease in PAM force, the shoulder pad profile has been designed to guarantee an increase in the PAM force lever arm in that range. At the same time, a significant reduction in the lever arm below 90° should be achieved. Unfortunately, this feature can't be granted by the shoulder pad. As a result, the user should make a considerable effort to move the arms below the horizontal, thus limiting the operating range of the exoskeleton only to flexion angles greater than 90° .

2.2 Configuration B: rotating cam-based transmission

In configuration B (Fig. 4), one end of the wire is still connected to the PAM lower end, and the other end runs inside a sheath fixed to the exoskeleton arm through a sheath clip (1) and then joins the cam (2). The latter, in turn, is integral with the strut (3) that sustains the bracelet (4). Therefore, the PAM contraction causes the cam rotation and, consequently, the elevation of the arm of the user.

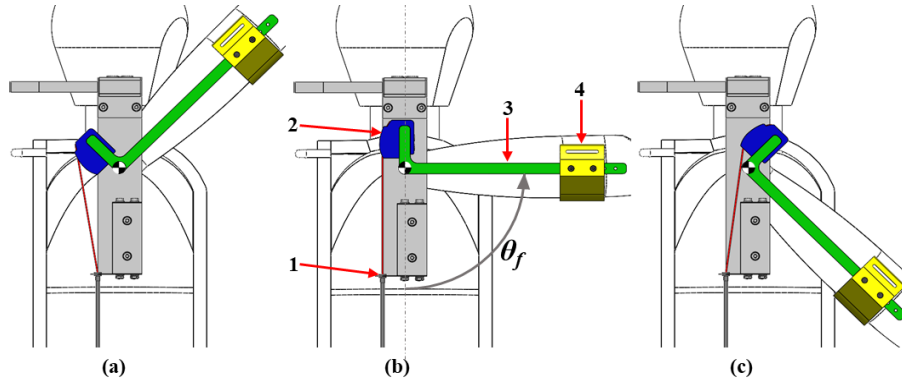


Fig. 4 Configuration B of the transmission shown for different shoulder flexion angles: (a) $\theta_f = 135^\circ$; (b) $\theta_f = 90^\circ$; (c) $\theta_f = 45^\circ$.

The cam adoption aims to extend the exoskeleton working range. As shown in Fig. 4c, the cam profile and its ability to rotate around the shoulder flexion axis both contribute to a significant reduction in the PAM force lever arm. The cam profile that minimizes the mismatch between the gravitational and assistive torque is again identified through a graphical approach, starting from the PAM lever arm values at 45° , 90° , and 135° . Given a defined supply pressure ($p = 4$ bar) and initial contraction ratio ($k_{90} = 0\%$), the PAM force lever arm at 90° shoulder flexion is obtained from the static equilibrium of the system, resulting in a 30 mm value. Then, the lever arm at 135° is set to 50 mm to achieve the required assisting torque without obstructing the user's view. Finally, the PAM lever arm at 45° is selected equal to 10 mm to obtain forces and contraction values that fall within the static PAM characteristic shown in Fig. 1.

The PAM stretching and lever arm are extrapolated from CAD design for six shoulder flexion angles ($45^\circ, 60^\circ, 75^\circ, 90^\circ, 105^\circ, 120^\circ, 135^\circ$) and interpolated over the working range. The results of this method for the rotating cam are shown in Fig. 5.

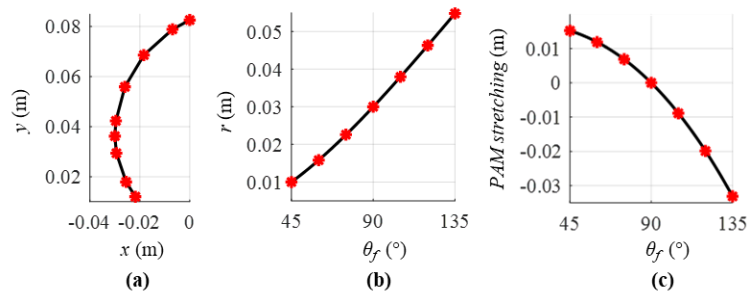


Fig. 5 Cam profile (a) along with the PAM force lever arm (b) and stretching (c) for shoulder flexion angles between 45° and 135° . The red dots are the data extrapolated from the CAD while the black line is the result of interpolation.

3 Simulations and Results

Accurate tuning of p and k_{90} can improve the match between gravitational (M_g) and assistive (M_{PAM}) torques. Values of p and k_{90} are varied between 4 bar and 5 bar and between 0% and 2%, respectively. The pressure range has been identified to ensure that the PAM traction force magnitude is adequate for the application, given the lever arms shown in Fig. 3(b) and Fig. 5(b). On the other hand, k_{90} greater than 2% is not considered to avoid excessive stroke reduction. Among the possible combinations of p and k_{90} , the one that minimizes the torque error expressed by Eq. (2) is chosen.

$$E = 100 \cdot \sqrt{\frac{1}{N} \sum_{i=\theta_m}^{135} \left(\frac{M_{PAM}(i) - M_g(i)}{M_g(i)} \right)^2} \quad (2)$$

θ_m is the minimum flexion angle achieved by the exoskeleton, and it is set to 90° and 45° for A and B configurations, respectively; N is the number of samples.

As shown in Fig. 6, the influence of the parameters on the torque error for each configuration is comparable. Regarding configuration B (Fig. 6(b)), the contraction ratio must be equal to 0.6% to minimize the torque error. Conversely, the error decreases as the contraction ratio increases in configuration A (Fig. 6(a)). The latter also requires a higher supply pressure.

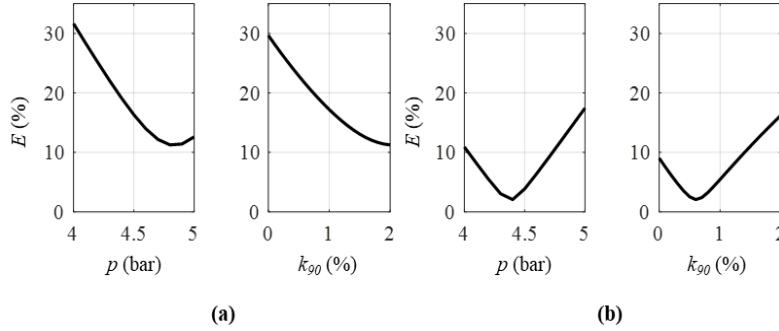


Fig. 6 Percentage error values between gravitational and assistive torque generated by configuration A (a) and B (b), obtained by varying optimization parameters.

The optimal (p, k_{90}) combination, one for each transmission solution, is then considered to evaluate the system performance in different conditions: unloaded condition, considering only the user's arm weight, and two loaded conditions, in which the user holds a tool of 1 or 2 kg in the hand (Fig. 7).

Fig. 7(a) shows that configuration A does not allow to reach shoulder flexion angles lower than 80° with a feasible approach. Below this value, the assistive torque that needs to be counteracted by the user can exceed five times the gravitational torque.

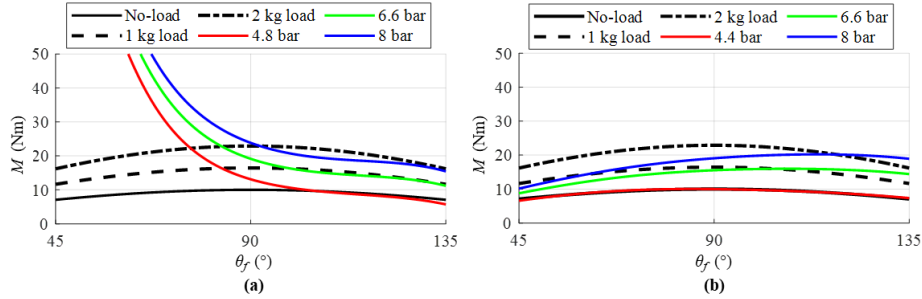


Fig. 7 Gravitational torque for different load conditions as well as the torque exerted by the exoskeleton at different supply pressures by employing A (a) and B (b) transmission design.

On the contrary, configuration B (Fig. 7(b)) allows accurate tracking of the gravitational torque in the unloaded condition, although the exoskeleton performance worsens by increasing the load in the hand. The percentage error, in fact, raises from 2% to 13%–20% of the gravitational torque when the load in the hand increases from 0 kg to 1–2 kg. Nonetheless, the exoskeleton support action is always higher than 80%, and the residual torque is low enough to be easily compensated by the user’s muscle action. It is likely that an appropriate regulation of supply pressure could further adapt the device behavior to different scenarios.

Regarding the mechanical strength of the system, some concerns are related to the fact that, for flexion angles lower than 60° , the maximum elongation of the PAM prescribed by the manufacturer (3%) is exceeded (3.7% if $\theta_f = 45^\circ$). This would likely result in unsafe conditions for the system, affecting long-term stability and reliability. However, that could be tackled by optimizing the design of the transmission or by searching for different PAMs (commercial or custom-made) with more appropriate features.

4 Conclusion

This work compared two different transmissions for a passive exoskeleton energized by pneumatic artificial muscles. In both solutions, within the respective operating ranges, the assistive torque of the exoskeleton compensates for more than 80% of the gravitational torque.

The design solution based on a cam rotating around the shoulder flexion axis proves to be more convenient regarding the operating range compared to the solution based on a fixed pad. On the other hand, the cam-based solution shows less adaptability to the presence of a load in the operator’s hand. Moreover, it requires placing the cam in a lateral position with respect to the shoulder, thus requiring the creation of a more complex and bulky structure and determining the arising of an abduction moment which is exerted on the user’s shoulder. Therefore, a future activity will concern the in-depth analysis of this solution in order to identify a possible ergonomic and compact configuration.

Regardless of the transmission adopted, the exoskeleton-human interaction forces should be investigated in the future to guarantee user safety and to achieve ergonomic behavior that helps improving the acceptance of such devices by workers. That should be attained by ensuring structural strength without unnecessary increase of device's weight and bulkiness.

Finally, a prototype of both transmissions should be developed to test their performance in a real-world scenario. In particular, the model neglected friction phenomena, device's weight, pneumatic losses, and PAM hysteresis. However, all these aspects could affect the actual behavior of the system.

References

1. Harib, O., Hereid, A., Agrawal, A., Gurriet, T., Finet, S., Boeris, G., Duburcq, A., Mungai, M.E., Masselin, M., Ames, A.D., Sreenath, K., Grizzle, J.W.: Feedback Control of an Exoskeleton for Paraplegics: Toward Robustly Stable, Hands-Free Dynamic Walking. *IEEE Control Syst.* 38, 61–87 (2018). <https://doi.org/10.1109/MCS.2018.2866604>.
2. Galle, S., Malcolm, P., Collins, S.H., De Clercq, D.: Reducing the metabolic cost of walking with an ankle exoskeleton: interaction between actuation timing and power. *J NeuroEngineering Rehabil.* 14, 35 (2017). <https://doi.org/10.1186/s12984-017-0235-0>.
3. Sun, M., Ouyang, X., Mattila, J., Yang, H., Hou, G.: One Novel Hydraulic Actuating System for the Lower-Body Exoskeleton. *Chin. J. Mech. Eng.* 34, 31 (2021). <https://doi.org/10.1186/s10033-021-00535-w>.
4. Ai, L., Zhou, T., Wu, L., Qian, W., Xiao, X., Guo, Z.: Design of a 6 DOF Cable-Driven Upper Limb Exoskeleton. In: Liu, X.-J., Nie, Z., Yu, J., Xie, F., and Song, R. (eds.) *Intelligent Robotics and Applications*. pp. 728–736. Springer International Publishing, Cham (2021). https://doi.org/10.1007/978-3-030-89095-7_69.
5. Trigili, E., Crea, S., Moise, M., Baldoni, A., Cempini, M., Ercolini, G., Marconi, D., Posteraro, F., Carrozza, M.C., Vitiello, N.: Design and Experimental Characterization of a Shoulder-Elbow Exoskeleton With Compliant Joints for Post-Stroke Rehabilitation. *IEEE/ASME Trans. Mechatron.* 24, 1485–1496 (2019). <https://doi.org/10.1109/TMECH.2019.2907465>.
6. Mauri, A., Lettori, J., Fusi, G., Fausti, D., Mor, M., Braghin, F., Legnani, G., Roveda, L.: Mechanical and Control Design of an Industrial Exoskeleton for Advanced Human Empowering in Heavy Parts Manipulation Tasks. *Robotics.* 8, 65 (2019). <https://doi.org/10.3390/robotics8030065>.
7. Bilancia, P., Berselli, G.: Conceptual design and virtual prototyping of a wearable upper limb exoskeleton for assisted operations. *Int J Interact Des Manuf.* 15, 525–539 (2021). <https://doi.org/10.1007/s12008-021-00779-9>.
8. Liu, C., Liang, H., Murata, Y., Li, P., Ueda, N., Matsuzawa, R., Zhu, C.: A wearable lightweight exoskeleton with full degrees of freedom for upper-limb power assistance. *Advanced Robotics.* 35, 413–424 (2021). <https://doi.org/10.1080/01691864.2020.1854115>.
9. Hyun, D.J., Bae, K., Kim, K., Nam, S., Lee, D.: A light-weight passive upper arm assistive exoskeleton based on multi-linkage spring-energy dissipation mechanism for over-

- head tasks. *Robotics and Autonomous Systems*. 122, 103309 (2019). <https://doi.org/10.1016/j.robot.2019.103309>.
10. Maurice, P., Camernik, J., Gorjan, D., Schirmeister, B., Bornmann, J., Tagliapietra, L., Latella, C., Pucci, D., Fritzsche, L., Ivaldi, S., Babic, J.: Objective and Subjective Effects of a Passive Exoskeleton on Overhead Work. *IEEE Trans. Neural Syst. Rehabil. Eng.* 28, 152–164 (2020). <https://doi.org/10.1109/TNSRE.2019.2945368>.
 11. Yin, P., Yang, L., Qu, S., Wang, C.: Effects of a passive upper extremity exoskeleton for overhead tasks. *Journal of Electromyography and Kinesiology*. 55, 102478 (2020). <https://doi.org/10.1016/j.jelekin.2020.102478>.
 12. Magnetti Gisolo, S., Muscolo, G.G., Paterna, M., De Benedictis, C., Ferraresi, C.: Feasibility Study of a Passive Pneumatic Exoskeleton for Upper Limbs Based on a McKibben Artificial Muscle. In: Zegloul, S., Laribi, M.A., and Sandoval, J. (eds.) *Advances in Service and Industrial Robotics*. pp. 208–217. Springer International Publishing, Cham (2021). https://doi.org/10.1007/978-3-030-75259-0_23.
 13. Paterna, M., Magnetti Gisolo, S., De Benedictis, C., Muscolo, G.G., Ferraresi, C.: A passive upper-limb exoskeleton for industrial application based on pneumatic artificial muscles. *Mech. Sci.* 13, 387–398 (2022). <https://doi.org/10.5194/ms-13-387-2022>.
 14. Piteř, J., Tóthová, M.: Modelling of pneumatic muscle actuator using Hill’s model with different approximations of static characteristics of artificial muscle. *MATEC Web Conf.* 76, 02015 (2016). <https://doi.org/10.1051/mateconf/20167602015>.